

# Exhibit 18

# **TRANSISTORS**

---

## **Fundamentals for the Integrated-Circuit Engineer**

By  
R.M. WARNER, Jr.  
Electrical Engineering Department  
University of Minnesota  
Minneapolis

B.L. GRUNG  
Corporate Technology Center  
Honeywell, Inc.  
Minneapolis



Robert E. Krieger Publishing Company  
Malabar, Florida  
1990

65972310  
ENGINEERING

*In appreciation of Mae, who made possible the completion of this work,  
and in memory of Margaret, who made possible its beginning.*

R.M.W.

*In appreciation of Sandy and Sonja for their continuous support.*

B.L.G.

Original Edition 1983  
Reprint Edition 1990 with corrections

Printed and Published by  
**ROBERT E. KRIEGER PUBLISHING COMPANY, INC.**  
**KRIEGER DRIVE**  
**MALABAR, FLORIDA 32950**

Copyright ©1983 by John Wiley and Sons, Inc.  
Reprinted by Arrangement

All rights reserved. No part of this book may be reproduced in any form or by any means, electronic or mechanical, including information storage and retrieval systems without permission in writing from the publisher.  
*No liability is assumed with respect to the use of the information contained herein.*  
Printed in the United States of America.

**Library of Congress Cataloging-in-Publication Data**  
**Warner, R.M.**

Transistors : fundamentals for the integrated  
circuit engineer.

Includes index.

1. Transistors. I. Grung, B.L. II. Title.  
TK7871.9W37 1990 621.3815'28 88-17417  
ISBN 0-89464-323-1

10 9 8 7 6 5 4 3 2

In work with silicon, and especially in MOS technology, it has become necessary to develop methods for achieving oxide-silicon interfaces of very low surface-recombination velocity, that is, less than 10 cm/s. At the other extreme, the realizable surface-recombination velocity can range up to higher than  $10^4$  cm/s. A lucid analysis and discussion of surface-recombination phenomena from the microscopic point of view has been offered by McKelvey [41]. He points out, quite plausibly, that the maximum achievable value of  $s$  is  $v_t/2$ , where  $v_t$  is the thermal velocity of the carriers involved. Nonetheless, it is quite common practice in the literature to assume for mathematical convenience an *infinite* value of  $s$  at a surface where one wants to preserve the values  $n_0$  and  $p_0$  strictly—to avoid excess carriers altogether. As McKelvey points out, this assumption of an unrealizable value for  $s$  does not lead to complications provided the diffusion velocity  $D_p/L_p \ll (v_t/2)$ . Using the numerical values employed in Section 3-4.2 (Case 2), where the diffusion-velocity idea was introduced, we find that  $D_p/L_p \approx 3.4 \times 10^3$  cm/s, while  $v_t/2$  is of order  $10^7$  cm/s, so that no problem is engendered in this typical case. In fact, situations that violate this condition are rare.

It has been common to characterize an ohmic contact to a semiconductor as a surface of infinite recombination velocity. In fact much of the attention paid to the surface-recombination phenomenon in the older literature was aimed at the nontrivial problem of ohmic-contact theory. Originally, ohmic contacts were made at intentionally damaged (e.g., sandblasted) surfaces. Today, however, an ohmic contact much more frequently involves a “high-low” junction. That is, to make an ohmic contact to an N region, one creates a very heavily doped, or “N<sup>+</sup>” region, adjacent to it and then makes metallic contact to this degenerate or nearly degenerate semiconductor. For this reason we shall satisfy ourselves with the brief phenomenological treatment of surface recombination given above, and examine in some detail the subject of high-low junctions in Chapter 6, partly for the sake of understanding ohmic contacts.

Having been introduced to the concept of surface-recombination velocity, the curious reader may wonder about conditions that were implicitly assumed at the irradiated surfaces invoked in this and the previous section. In fact, there is evidence that irradiation alters (lowers) effective surface-recombination velocity [42], a point that has an important bearing on solar-cell performance. This phenomenon does not alter the validity of the descriptions offered above, however, because all that was required in those steady-state problems was a mechanism for providing a source of excess carriers in the leftward portion of the sample.

### 3-5 DEVIATIONS FROM NEUTRALITY

All of the foregoing discussion in this chapter has dealt with important cases wherein neutrality is preserved. Such cases can, in fact, be regarded as the norm in “bulk” samples, where we interpret this term to mean “a long way

### 6-3.4 Applying Fletcher Boundary Conditions to a High-Low Junction

Let us arbitrarily select an  $NN^+$  junction for examination. The question that then arises is, "Can the boundary-density expressions developed in Section 6-3.1, or different expressions similarly derived, be applied to such a junction?" The answer is that the equations already derived can be applied, provided we make a proper symbol identification in the process of transition from the PN case to the  $NN^+$  case, an approach that was employed by Grung and Warner [12]. To see this, consider the sequence of junctions in Fig. 6-14. At the top is shown a sample where the right-hand side is permanently  $N^+$ , but the left-hand side has (in a thought experiment, to be sure) variable doping. In Fig. 6-14*b* is represented a  $PN^+$  junction that may without any equivocation be regarded as the PN junction for which the derivation of Fletcher boundary conditions in Section 6-3.1 was developed. What limitations, if any, exist on the applicability of the four boundary-density expressions that resulted there, to the  $IN^+$  and  $NN^+$  junctions depicted in Figs. 6-14*c* and 6-14*d*, respectively? The assumptions of Boltzmann quasiequilibrium and of neutrality at the

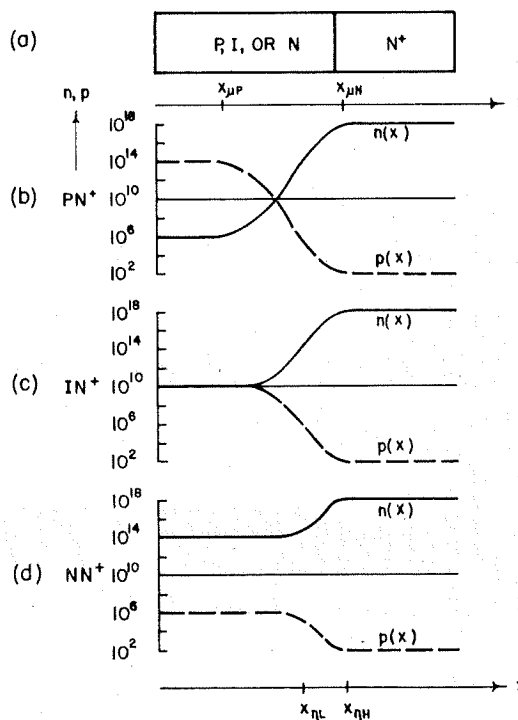


**Figure 6-14** Step-junction sample with "variable" left-hand doping for illustrating Fletcher-boundary-condition applicability. (a) Physical representation. (b) Semilog carrier profiles for  $PN^+$  junction. (c) Semilog carrier profiles for  $IN^+$  junction. (d) Semilog carrier profiles for  $NN^+$  ("low-high") junction.



## 6-3 HIGH-LEVEL JUNCTION THEORY

447

boundaries apply equally well to all three samples, so no limitation is engendered there. Next, examine the neutrality expressions, Eqs. (6-72) and (6-73). Both are symmetric, so that they inject no preference with respect to holes or electrons, or with respect to majority or minority carriers, into the problem.

Now consider the Boltzmann expressions, Eqs. (6-65) and (6-66). We want to be certain that we are addressing forward bias, which is to say, bias of such a sense that the equilibrium built-in potential step is diminished in height. The reason for this restriction is that forward- and reverse-bias behavior are qualitatively different in a PN junction, as shown in Section 6-2.1, and Fletcher boundary conditions apply in forward bias. Once a sign convention has been adopted, and we have made quite a point of our preferred convention, then Eqs. (6-65) and (6-66) are valid so long as

$$p(x_{\mu P}) > p(x_{\mu N}) \quad (6-121)$$

and

$$n(x_{\mu P}) < n(x_{\mu N}). \quad (6-122)$$

Now observe that all three examples in Fig. 6-14 fit these inequalities. Thus the existing equations can be applied by treating the  $N^+$  region as the "N side" and the N region as the "P side," or analogous to it because it is less N-type.

To this end, simply let the boundary locations on the "low" and "high" sides, respectively, be designated  $x_{\eta L}$  and  $x_{\eta H}$ , as shown in Fig. 6-14d. Then Eq. (6-83) is converted into

$$p(x_{\eta L}) = \frac{(p_{0L} - n_{0L})n_{0H}p_{0L} + (n_{0H} - p_{0H})n_{0L}p_{0L}\exp\frac{q(-V_J)}{kT}}{n_{0H}p_{0L} - n_{0L}p_{0H}\left(\exp\frac{q(-V_J)}{kT}\right)^2} \quad (6-123)$$

Now since  $p_{0H} \ll n_{0H}$ , the simplification

$$p(x_{\eta L}) \approx \frac{(p_{0L} - n_{0L})n_{0H}p_{0L} + n_{0H}n_{0L}p_{0L}\exp\frac{q(-V_J)}{kT}}{n_{0H}p_{0L} - n_{0L}p_{0H}\left(\exp\frac{q(-V_J)}{kT}\right)^2} \quad (6-124)$$

is justified. Next, divide numerator and denominator by  $n_{0H}p_{0L}$ , so that

$$p(x_{\eta L}) = \frac{p_{0L} - n_{0L} + n_{0L} \exp \frac{q(-V_J)}{kT}}{1 - \frac{n_{0L}p_{0H}}{p_{0L}n_{0H}} \left( \exp \frac{q(-V_J)}{kT} \right)^2}$$

$$= \frac{p_{0L} + n_{0L} \left[ \left( \exp \frac{q(-V_J)}{kT} \right) - 1 \right]}{1 - \frac{n_{0L}p_{0H}}{p_{0L}n_{0H}} \left( \exp \frac{q(-V_J)}{kT} \right)^2}. \quad (6-125)$$

Next, consider that  $n_{0L} \approx N_{DL}$ , and  $n_{0H} \approx N_{DH}$ , so that

$$p(x_{\eta L}) = \frac{p_{0L} + N_{DL} \left[ \left( \exp \frac{q(-V_J)}{kT} \right) - 1 \right]}{1 - \frac{N_{DL}^2}{n_i^2} \frac{n_i^2}{N_{DH}^2} \left( \exp \frac{q(-V_J)}{kT} \right)^2}, \quad (6-126)$$

or

$$p(x_{\eta L}) = \frac{p_{0L} + N_{DL} \left[ \left( \exp \frac{q(-V_J)}{kT} \right) - 1 \right]}{1 - \left( \frac{N_{DL}}{N_{DH}} \right)^2 \left( \exp \frac{q(-V_J)}{kT} \right)^2}. \quad (6-127)$$

To achieve a first quantitative assessment of the difference in behavior of high-low junctions and PN junctions, let us inquire about the magnitude of the imposed junction voltage in forward bias,  $-V_J$ , required to produce a 1000-fold increase in the boundary value  $p(x_{\eta L})$ . Recall from the discussion of low-level bias in connection with Fig. 6-4 that a terminal voltage of 0.173 V was required to accomplish this in a PN junction. We shall find that a far lower voltage is required in the high-low junction. Anticipating a bit, or applying the iterative technique, if one prefers, let us simplify Eq. (6-127) somewhat further. Since the factor  $(N_{DL}/N_{DH})^2$  in the second term of the denominator equals  $10^{-8}$  in the present example, it follows that for the small value of  $V_J$  that will be calculated below, Eq. (6-127) can be rewritten as

$$p(x_{\eta L}) \approx p_{0L} + N_{DL} \left[ \left( \exp \frac{q(-V_J)}{kT} \right) - 1 \right]. \quad (6-128)$$

## 6-3 HIGH-LEVEL JUNCTION THEORY

449

Thus,

$$-V_J = \frac{kT}{q} \ln \left( \frac{p(x_{\eta L}) - p_{0L}}{N_{DL}} + 1 \right). \quad (6-129)$$

Hence, in the case assumed,

$$-V_J = \frac{kT}{q} \ln \left( \frac{999p_{0L}}{N_{DL}} + 1 \right) = 2.5 \times 10^{-7} \text{ V}, \quad (6-130)$$

since in the  $NN^+$  junction of Fig. 6-14d,  $p_{0L}/N_{DL} = 10^{-8}$ . Comparing the result for this particular high-low junction with that previously obtained for a PN junction indicates that the ratio of the imposed junction voltages (PN versus high-low) required to inflate the minority-carrier densities on their low sides by a factor of 1000 is

$$\frac{V_J(PN, 1000)}{V_J(HL, 1000)} = 6.9 \times 10^5. \quad (6-131)$$

In short, the high-low junction is much more "sensitive" to imposed junction voltage in the respect examined than is the PN junction. The reason for this difference is prominently displayed in Eq. (6-128), wherein the exponential voltage-dependent factor multiplies (in effect) the equilibrium *majority* density, rather than the minority density as in a PN junction.

To show that the  $p(x_{\eta L})$  result is essentially the same for either Eq. (6-127) or Eq. (6-128), substitute Eq. (6-130) into the denominator of Eq. (6-127), yielding

$$1 - \left( \frac{N_{DL}}{N_{DH}} \right)^2 \left( \exp \frac{q(-V_J)}{kT} \right)^2 = 0.99999999. \quad (6-132)$$

Thus, taking the denominator of Eq. (6-127) to be unity constitutes an extremely mild approximation. The result in Eq. (6-132) further shows that  $V_J$  and  $p(x_{\eta L})$  are quite independent of high-side doping, so long as a few decades of doping difference exist between the high and low sides. Low-side doping is primary, as Eq. (6-130) shows. The first term in the argument of the logarithm goes as  $p_{0L}/N_{DL}$ , and hence essentially as  $1/N_{DL}^2$ . Thus the magnitude of  $V_J$  increases as  $N_{DL}$  decreases, but its dependence is logarithmic and quite slow.

In spite of the "sensitivity" of  $p(x_{\eta L})$  to  $V_J$ , the fact of extremely low  $V_J$  magnitude means that  $p(x_{\eta L})$  remains small compared to  $n(x_{\eta L})$ . In other words, forward-biasing a high-low junction, even at high levels, does not cause conductivity modulation in the low region. This is one of the properties of a high-low junction that makes it so useful as an ohmic contact. A second important property of an ideal ohmic contact is that it exhibits negligible



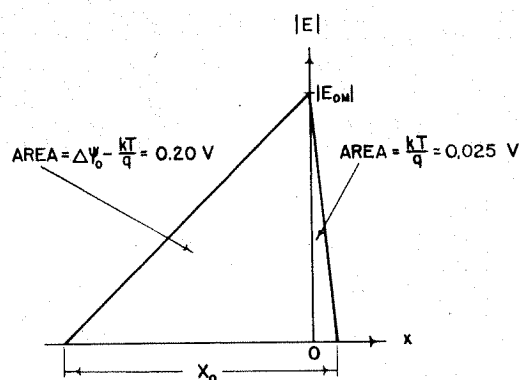


Figure 6-15 Simplified equilibrium field profile for junction of Fig. 6-14d.

resistance. The high-low junction can be tested on this score by means of a further calculation. Let us show that a high-low junction conducts a huge current density with very small  $V_j$ . In other words, the junction itself “absorbs” a very small fraction of an applied voltage. Because of this property, ohmic drop in the “low” region is typically more of a limitation than voltage absorbed in the transition region of a high-low junction.

To carry out an order-of-magnitude calculation, let us employ information from the general solution, Section 5-6, in combination with principles employed in the depletion approximation. The term “depletion approximation” is hardly appropriate here because depletion exists only on the high side of a high-low junction; the bulk of the voltage drop in the transition region of a high-low junction is, in fact, associated with carrier *accumulation* on the low side. But nonetheless, depletion-approximation principles remain valid. In Fig. 6-15 is shown a simplified equilibrium field profile for the  $NN^+$  junction of Fig. 6-14d. From Eq. (5-149) we know that normalized field at such a junction (normalized in terms of the high side) is given by  $|dW/d(x/L_D)| = \sqrt{2/e}$ . Consequently, peak field is given by

$$E_{0M} = \frac{kT}{q} \frac{1}{L_{DH}} \sqrt{\frac{2}{e}} = \sqrt{\frac{kT}{q} \frac{qN}{\epsilon} \frac{2}{e}} = 5.27 \times 10^4 \text{ V/cm.} \quad (6-133)$$

Since normalized-potential drop on the high side (or  $W$ , in terms of the Section 5-6 formulation) is one unit, from Eq. (5-151) it follows that

$$n(0) = \frac{n_{0H}}{e} \approx \frac{N_{DH}}{e}. \quad (6-134)$$

Knowledge of both  $n(0)$  and  $E(0) = E_{0M}$  permits a calculation of the drift component of electron current at  $x = 0$ , that is, at the junction. Figure 3-7 indicates that for the value of  $E_{0M}$  just calculated, a mobility value of 200

## 6-3 HIGH-LEVEL JUNCTION THEORY

451

$\text{cm}^2/\text{V s}$  is appropriate for an approximate calculation. Hence

$$J_{n,\text{drift}}(0) = q\mu_n n(0) E_{0M} = 6.2 \times 10^5 \text{ A/cm}^2. \quad (6-135)$$

Let our approach be as follows: Assume an imposed junction voltage in the forward direction of the magnitude computed above, and then estimate what net current density passing through the junction would be associated with it.

First, note that the total voltage drop in the high-low junction at equilibrium can be written, from the Boltzmann relation, Eq. (3-51), as

$$\Delta\psi_0 = \frac{kT}{q} \ln \frac{n_{0H}}{n_{0L}} = 0.23 \text{ V}. \quad (6-136)$$

As a matter of curiosity, let us calculate  $X_0$  as well, the approximate thickness of the transition region. Combining the results in Eqs. (6-133) and (6-136) in the manner made evident by Fig. 6-16 yields

$$X_0 = 2 \frac{\Delta\psi_0}{E_{0M}} = 9 \times 10^{-6} \text{ cm} \approx 0.1 \text{ } \mu\text{m}. \quad (6-137)$$

Evidently this dimension is small. The transition region consists of a thin accumulation layer on the low side, and an even thinner depletion layer on the high side.

Next, let the potential step of the high-low junction be diminished by the amount given in Eq. (6-130); the fractional reduction then amounts to

$$\left| \frac{V_{J(HL,1000)}}{\Delta\psi_0} \right| = 1.1 \times 10^{-6} \equiv \delta, \quad (6-138)$$

so that the height of the potential step under forward bias is

$$\Delta\psi = \Delta\psi_0(1 - \delta). \quad (6-139)$$

Now, since  $E_{0M}$  is the altitude of the triangle in Fig. 6-15, and  $\Delta\psi_0$  is its area, it follows that the relative change in peak field because of the applied bias varies as the square root of the relative change in the height of the potential step, or

$$\frac{E_M}{E_{0M}} = \left( \frac{\Delta\psi}{\Delta\psi_0} \right)^{1/2} = (1 - \delta)^{1/2}. \quad (6-140)$$

Employing the binomial approximation, then

$$E_M \approx E_{0M} \left( 1 - \frac{\delta}{2} \right). \quad (6-141)$$

When a junction is subjected to an increment of forward bias, the diffusion component of current at the metallurgical junction is enhanced and the drift component is diminished, and the sum of these incremental magnitudes constitutes the net current. A qualitative argument based on Fig. 6-15 makes this inevitable result plausible: Reducing the area of the triangle reduces  $E_M$  and  $X$ , with the former responsible for reduced drift current. In spite of the reduction in  $X$ , the electron density must still make a transition from essentially  $N_{DH}$  to  $N_{DL}$ , just as it did at equilibrium. The fact that this now occurs in a smaller interval  $X$  means that  $dn/dx$  has increased, and so the diffusion component of current increases.

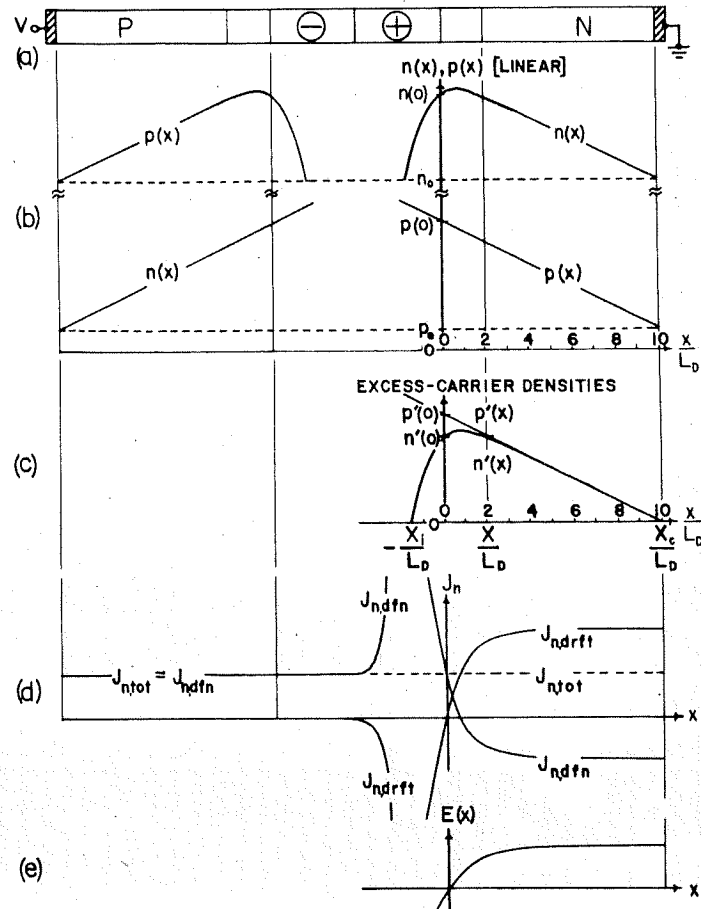


**Figure 6-16** Modeling the boundary region of a forward-biased junction (after Warner and Lee [22]). (a) Physical representation of symmetric step junction with infinite lifetimes and ideal ohmic contacts. (b) Carrier profiles with low-level forward bias applied and with  $X_c = 10L_D$ . (c) Excess-carrier profiles under same conditions. (d) Qualitative electron-current-component distributions. (e) Field profile exhibiting the field reversal that is employed to define the spatial origin for the analytical solution.



## 6-3 HIGH-LEVEL JUNCTION THEORY

453

For purposes of the order-of-magnitude calculation, let us assume that the drift- and diffusion-current components contribute equally to the net current. (Note that hole current can be neglected in the  $NN^+$  case, so that only the two components of electron current concern us.) As a result then, the net current will be twice the increment introduced by the field change, or

$$J_{n,\text{net}}(0) \approx 2\left(\frac{\delta}{2}\right) J_{0n,\text{drft}}(0) = 0.7 \text{ A/cm}^2. \quad (6-142)$$

Thus for an imposed junction voltage of about  $0.25 \mu\text{V}$  as computed in Eq. (6-130), there results a significant current density. The practical upper limit on current-density values one could expect to encounter in device situations might be two (or at most three) decades higher than that computed in Eq. (6-142), so that even there the imposed junction voltage in a high-low junction of the kind assumed here would be far less than  $1 \text{ mV}$ .

We have seen that conductivity modulation does not occur on the low side, and it is intuitively reasonable that it does not occur on the high side either, since even in a one-sided PN junction the high side is essentially "immune" to the effect. Therefore the majority densities at the boundaries,  $n(x_{\eta L})$  and  $n(x_{\eta H})$ , can be regarded as approximately constant and approximately equal to  $N_{DL}$  and  $N_{DH}$ , respectively. For completeness in the present task, however, let us calculate the minority-hole density on the high side. Proceeding in a manner like that used for the low side, start with Eq. (6-81). Substituting notation appropriate to the high-low junction yields

$$p(x_{\eta H}) = \frac{(p_{0L} - n_{0L})n_{0H}p_{0H}\exp\frac{q(-V_J)}{kT} + (n_{0H} - p_{0H})n_{0L}p_{0H}\left(\exp\frac{q(-V_J)}{kT}\right)^2}{n_{0H}p_{0L} - n_{0L}p_{0H}\left(\exp\frac{q(-V_J)}{kT}\right)^2}. \quad (6-143)$$

Because  $p_{0H} \ll n_{0H}$  this becomes

$$p(x_{\eta H}) \approx \frac{(p_{0L}n_{0H}p_{0H} - n_{0L}n_{0H}p_{0H})\exp\frac{q(-V_J)}{kT} + n_{0H}n_{0L}p_{0H}\left(\exp\frac{q(-V_J)}{kT}\right)^2}{n_{0H}p_{0L} - n_{0L}p_{0H}\left(\exp\frac{q(-V_J)}{kT}\right)^2}. \quad (6-144)$$



Divide numerator and denominator by  $p_{0L}n_{0H}$ :

$$p(x_{\eta H}) \approx \frac{\left(p_{0H} - \frac{n_{0L}p_{0H}}{p_{0L}}\right) \exp \frac{q(-V_J)}{kT} + \frac{n_{0L}p_{0H}}{p_{0L}} \left(\exp \frac{q(-V_J)}{kT}\right)^2}{1 - \frac{n_{0L}p_{0H}}{p_{0L}n_{0H}} \left(\exp \frac{q(-V_J)}{kT}\right)^2} \quad (6-145)$$

Using arguments analogous to those employed for  $p(x_{\eta L})$ , Eq. (6-145) can then be reduced to

$$p(x_{\eta H}) \approx p_{0H} \exp \frac{q(-V_J)}{kT} + \frac{N_{DL}^2}{N_{DH}} \left(\exp \frac{q(-V_J)}{kT}\right) \left[\left(\exp \frac{q(-V_J)}{kT}\right) - 1\right] \quad (6-146)$$

Comparing Eqs. (6-146) and (6-128) reveals interesting differences between these approximate expressions. The low-side hole density  $p(x_{\eta L})$  depends on low-side properties only. Also, the first term is unmodulated by  $V_J$ . But  $p(x_{\eta L})$  has a first term that is so modulated. This is because holes can "spill over" from the low side where they are (in this example)  $10^4$  times more abundant. Also,  $p(x_{\eta H})$  has a value that is a function of doping on both sides. We noted in connection with asymmetric PN junctions that the low side plays the most important role in determining junction properties. In the high-low case, the points just made suggest that the low side is once more dominant.

All discussion thus far has centered on the case of forward bias. In reverse bias, the potential barrier grows, as in PN junction, but only by a very small amount. The dominant transport mechanism in the transition region of the high-low junction is drift. Thus low-region electrons that approach the junction in reverse bias are swept through readily. (Recall that in forward bias, electrons spill over from the high region and move the other way in the low region.) Consequently, the high-low junction exhibits the low resistance so urgently desired in an ohmic contact when it is in reverse bias, as well as forward bias. As quantitative demonstration that the Fletcher boundary conditions are not applicable in reverse bias, one can apply a reverse bias of  $0.25 \mu\text{V}$  to the high-low junction assumed at the beginning of this section. In this case, the approximate Eq. (6-128) yields an absurd result—a negative hole density. The minority-hole density on the low side is, however, significantly depressed for reverse bias, a point we will examine in Section 8-5.5 where a high-low junction is incorporated in a bipolar transistor.

Summing up, we can say that majority carriers are able to move easily through a high-low junction in either direction, with the direction of transport depending upon bias polarity. Because of this ready conduction in either

#### 6-4 ANALYSIS OF A PARTICULAR JUNCTION UNDER FORWARD BIAS 455

direction in response to very small applied voltage, a high-low junction constitutes a convenient and efficient ohmic contact to a semiconductor region, even when that region is quite lightly doped.

#### 6-4 DETAILED ANALYSIS OF A PARTICULAR JUNCTION UNDER FORWARD BIAS

The PN junction poses analytical difficulties even at equilibrium, as noted in Chapter 5, and so the forward-biased case that interests us here is even more challenging. Because of such difficulties, the junction has been the subject of numerous and extensive numerical calculations [13–19]. Our approach will combine a numerical solution for the deeply depleted region near the junction with an exact analytical solution for the boundary region of the transition layer, a solution made possible by simplifying assumptions concerning the device and its properties.

##### 6-4.1 Structure to Be Modeled

Analytical models of biased junctions have been offered previously. Middlebrook [20] has presented analytical approximations for the reverse-biased junction—specifically for the case of the collector junction of a bipolar transistor in normal operation. As noted in connection with Fig. 6-6c, however, a field reversal exists at both boundaries of a forward-biased junction. This fact provides a point of entry for analysis because the transport of both carrier types is purely diffusive at these surfaces. Guckel et al. [21] have previously exploited the existence of these zero-field surfaces to treat the abrupt junction under forward bias. Subsequently, Warner and Lee [22] did so also, and we shall follow the latter analysis. The two treatments differ in two major respects. Guckel et al. focused primarily on the region of significant depletion, or depletion and inversion, in the case of an asymmetric junction, that lies near the metallurgical junction. Warner and Lee focused on the region at the boundary of the space-charge layer and to a lesser degree on the adjacent quasineutral region that extends all the way to the corresponding ohmic contact. The first group of authors produced approximate analytical solutions for a wide range of doping relationships in the abrupt junction, while the second group made simplifying assumptions and then have provided an exact analytical solution for the boundary and quasineutral regions. The analysis below thus does not have general applicability because of its restrictive assumptions, but nonetheless it does provide a kind of modeling insight into the behavior of carrier populations that is very difficult to extract from purely numerical studies, and even from approximate analytical studies.

The zero-field surfaces whose presence we exploit exist for any forward bias, high or low. But as the first (and major) simplification, we shall assume